Ab Initio Study of the $CH_3F\cdots H_2O$ Complex†

Jeremy E. Monat, Rafał R. Toczyłowski, and Sławomir M. Cybulski*

Department of Chemistry and Biochemistry, Miami University, Oxford, Ohio 45056

Received: April 6, 2001; In Final Form: July 9, 2001

The $CH_3F\cdots H_2O$ complex has been studied using both the supermolecule approach through fourth-order Møller−Plesset perturbation theory (MP4) and perturbation theory of intermolecular forces. Nine configurations have been examined, seven of which were found to be attractive. The global minimum occurs when a bent C−F···H−O hydrogen bond is formed with the C···O distance of 6.15 a_0 and the water molecule in the same plane as the hydrogen bond. The binding energy for this geometry is equal to 5291 μE_h (3.32 kcal/mol) at the MP4 level of theory. When bond functions are included in the basis set, this configuration is further stabilized to 5739 μE_h (3.60 kcal/mol). The two configurations where a hydrogen atom of water is closest to the carbon atom of fluoromethane are repulsive at all distances examined due to electrostatic interactions. The increase of the magnitude of the binding energy when the basis set includes bond functions is primarily due to increased attractiveness of dispersion energy. The electrostatic interaction is the most significant energy component for all seven attractive configurations at their radial minima, particularly for configurations where the C−F bond points toward the H_2O molecule. The exchange and dispersion energies are, respectively, the second and third most important contributions to the interaction energy for the seven attractive configurations at their radial minima. The MP2 interaction energy is found to approximate the MP4 interaction energy qualitatively, but underestimates the attraction of the seven attractive configurations at their optimal intermolecular separations by 8−82 μE_h. A model potential for the $CH_3F\cdots H_2O$ system has been developed.

I. Introduction

Jeffrey and Saenger in their monograph on hydrogen bonding[1] noted that the literature contained "very few references to X−H···F−C bonds" even though the biological activity of C−F-containing compounds has been known since 1944 when Marais[2] reported the isolation of fluoroacetic acid from a poisonous South African plant. Fluoroacetate, itself innocuous, is converted by the enzyme citrate synthase into a toxic fluorocitrate which competitively inhibits and inactivates the critical enzyme aconitase ultimately resulting in the death of an animal which consumed leaves of the plant.[3] X-ray crystallography has shown that a bent C−F···H−O hydrogen bond exists for fluorocitrate esters.[4] However, questions have been raised as to whether this arrangement is the most energetically favorable or is a result of steric factors in the crystal lattice. Furthermore, whether the C−F···H−O interaction in 2-fluoroethanol and related systems is a hydrogen bond has been debated in several works.[5−9] Various spectroscopic techniques[10−15] demonstrated that 2-fluoroethanol exists largely in the gauche configuration in both the liquid and the gas phase which supported the existence of an intermolecular hydrogen bond. However, Griffith and Roberts showed,[16] using proton NMR, that the chemical shift of the methylene protons did not vary with solution concentration, nor was the hydroxylic proton significantly deshielded. They therefore concluded that the C−F···H−O interaction was too weak to be a hydrogen bond.

More recently, the presence of the C−F···H−N hydrogen bonds has been observed in a study of DNA replication.[17] It was found that the difluorotoluene nucleoside did not form a C−F···H−N hydrogen bond with adenine derivatives even in chloroform, which tends to stabilize hydrogen bonds.[18,19] Nevertheless, the difluorotoluene nucleoside coded for adenine quite efficiently. The degree to which energetics, in tandem with geometry, helps the difluorotoluene nucleoside substitute for thymine is not yet entirely clear although ab initio calculations of Ryjáček et al.[20] show that planar hydrogen bonded complexes of difluorotoluene and adenine are significantly weaker than the complexes of thymine and adenine.

Apart from the work of Ryjáček et al. there were several other ab initio studies concerned with C−F···H−X hydrogen bonds. Tarakeshwar et al.[21] reported the results for fluorobenzene···water and difluorobenzene···water complexes, and Caminati et al.[22] examined the difluoromethane···water complex. Ab initio calculations for difluoromethane···water as well as fluoromethane···water complexes have been reported by Howard et al.[23] Finally, mention should also be made of the works of Veenstra et al.[24] as well as Alkorta and Maluendes[25] who examined the interaction of fluorocarbons with water. The C−F···H−O hydrogen bond was not examined in these studiesas they were both focused on the C−H···O hydrogen bond. The results of Alkorta and Maluendes[25] obtained using fourth-order Møller−Plesset perturbation theory (MP4) and the 6-31++G(d,p) basis set are more accurate, giving the binding energy of 2200 μE_h in their Approach A.

In the present study, we examine the $CH_3F\cdots H_2O$ complex, which we view as a model system for determining the stability of the intermolecular C−F···H−O hydrogen bond. The interaction between CH_3F and H_2O is also of interest as an extension of the alkane···water interaction. The latter is a classic example of a nonpolar···polar interaction. Fluoromethane, however, is a polar analogue of methane and is expected to interact with water differently, especially when the electrostatic implications of the C−F bond dipole are considered. The $CH_4\cdots H_2O$

† This paper is dedicated to the memory of Professor Anastas Karipides (1937−1994).

10.1021/jp011279o CCC: $20.00
Published on Web 09/07/2001

interaction has already been studied theoretically and experimentally. At the MP4 level of theory, the most attractive geometry of $CH_4\cdots H_2O$ occurred when a C···H−O hydrogen bond was formed and the C···O separation was 6.8 a_0.[26] This finding was corroborated by pulsed-nozzle Fourier transform microwave spectrum of the complex[27] which indicated that the zero-point center-of-mass separation is approximately 7.0 a_0. Further isotopic studies[27] showed that a proton is donated from the hydrogen of water to CH_4 in a slightly nonlinear C···H−O hydrogen bond.

In this study, the $CH_3F\cdots H_2O$ system is studied using the supermolecule approach up to fourth-order of Møller−Plesset perturbation theory (MP4). Simultaneous calculations of energy components are also performed using perturbation theory of intermolecular forces. The interaction energy and its components are examined as functions of intermolecular geometry. The effects of including bond functions are investigated, and a model potential is developed. All quantities reported in this work are given in atomic units: distances in a_0 and energies in μE_h. Where necessary, the literature values were converted to these units.

II. Methods and Definitions

The supermolecule interaction energies at the SCF level of theory, ΔE^{SCF}, and at the nth order of Møller−Plesset perturbation theory, ΔE^{MPn}, can be related to the intermolecular Møller−Plesset perturbation theory (IMPPT) component energies.[28] The latter represent physically meaningful terms contributing to the interaction energy, such as electrostatics, induction, dispersion, and exchange.[28] Such components are designated as $\epsilon^{(ij)}$, where i and j are the orders of the corrections with respect to the intermolecular interaction and intramolecular correlation operators, respectively. In the present work, we limit our analysis to the SCF and MP2 levels of theory since partitioning of ΔE^{MP3} and ΔE^{MP4}, even though it has been described,[29,30] remains to be implemented.

A. Partitioning of ΔE^{SCF}. The ΔE^{SCF} energy is composed of electrostatic, exchange, and deformation components.[29−31]

$$\Delta E^{SCF} = \Delta E^{HL} + \Delta E^{SCF}_{def} \quad (1)$$

$$\Delta E^{HL} = \epsilon^{(10)}_{es} + \epsilon^{HL}_{ex} \quad (2)$$

The electrostatic energy, $\epsilon^{(10)}_{es}$, describes interactions of the two molecules' permanent moments and charge overlap effects. The exchange energy, ϵ^{HL}_{exch}, accounts for the repulsion of electrons on opposing molecules.[32] Their sum is known as the Heitler−London energy, ΔE^{HL}. The SCF deformation energy, ΔE^{SCF}_{def}, is a quantum induction term which takes into account both classical induced moments and exchange effects. By contrast, the second-order induction energy, $\epsilon^{(20)}_{ind,r}$, includes only classical induction.

The coupled Hartree−Fock (CHF) induction energy series

$$\epsilon^{CHF}_{ind,r} \cong \epsilon^{(20)}_{ind,r} + \epsilon^{(30)}_{ind,r} + ... + \epsilon^{(n0)}_{ind,r} + ... \quad (3)$$

was found to be divergent, so we will examine only its first term, $\epsilon^{(20)}_{ind,r}$, which has been useful in modeling.[33] It can be treated as an exchangeless approximation to the deformation energy.

B. Partitioning of $\Delta E^{(2)}$. The second-order correlation correction can be dissected as follows:

$$\Delta E^{(2)} = \epsilon^{(12)}_{es,r} + \epsilon^{(20)}_{disp} + \Delta E^{(2)}_{def} + \Delta E^{(2)}_{ex} \quad (4)$$

where $\epsilon^{(12)}_{es,r}$ is the second-order electrostatic correction energy with response effects[31] and $\epsilon^{(20)}_{disp}$ is the second-order dispersion energy.[32] $\Delta E^{(2)}_{def}$ and $\Delta E^{(2)}_{ex}$ are, respectively, the second-order deformation correlation correction to the SCF deformation and the second-order exchange correlation.

C. Interaction Energy Calculations. Unless stated otherwise, all calculations were performed in the basis set of the dimer,[34−38] which is equivalent to using the counterpoise procedure of Boys and Bernardi to eliminate basis set superposition error (BSSE).[39] The experimentally determined monomer geometries were assumed to be frozen during the interaction. For CH_3F, the experimental parameters of Duncan[40] were used: the C−F and C−H bond lengths were 2.612 and 2.069 a_0, respectively, and the H−C−H angle was 110.5°, giving an F−C−H angle of 108.6°. For H_2O, the parameters of Benedict et al.[41] were used: the O−H bond length was 1.809 a_0 and the H−O−H angle was 104.52°. The use of frozen monomer geometries was the necessary approximation that allowed us to focus on the intermolecular degrees of freedom in the development of the intermolecular potential for the $CH_3F\cdots H_2O$ complex. Such an approximation is justified since it is well-known that geometries of monomers in weakly interacting complexes undergo only small changes. For example, in the HF dimer, the intramolecular H−F bonds were found to change by only 0.004−0.006 a_0 compared to the H−F bond length in an unperturbed molecule.[42]

The calculations were carried out with *Gaussian94*[43] and *Molpro2000*[44] programs and *Trurl 98*[45] IMPPT package.

D. Basis Sets. In all cases, Sadlej's (10s6p4d/6s4p)/[5s3p2d/3s2p] basis set[46,47] was used as a minimum. It has two sets of doubly contracted polarization functions on all nuclei, but is still relatively small. Nonetheless, its accuracy in calculations of electric properties is on a par with larger basis sets.[46,47] The frozen core approximation was employed at only the MP3 and MP4 levels of theory since its use affected the MP2 interaction energy by less than 1%.

Sadlej's basis sets, with their lack of orbitals with symmetry higher than d, tend to underestimate the dispersion energy.[26,48] To saturate the dispersion energy more fully, in some calculations a set of bond functions[49−51] was used. It comprised three sp orbitals with exponents 0.9, 0.3, and 0.1 and two d-symmetry orbitals with exponents 0.6 and 0.2.[51]

III. Results and Discussion

A. Properties of the Monomers. To aid in the development of a potential, properties of the isolated fluoromethane and water monomers were calculated in the basis sets of the monomers. The SCF and MP2 values were calculated analytically, and the MP4 values were determined using the finite field method (field strength ±0.001 au) since analytic codes were not available. Results are shown in Tables 1 and 2. For all properties, we adopt the spherical tensor notation and denote multipole moments by Q_{lm}, and polarizabilities by $\alpha^{ll'}_{mm'}$. Literature values are given for comparison; extensive compilations of earlier results may be found in the quoted sources. Values presented in Tables 1 and 2 are typically in good agreement with those reported by other workers despite our smaller basis set. For both molecules, the dipole moment, Q_{1m}, the quadrupole moment, Q_{2m}, and the dipole polarizability, $\alpha^{11}_{mm'}$, are close to the accepted theoretical and experimental values.[52−62] We did not find any literature data for dipole−quadrupole, $\alpha^{21}_{mm'}$, and quadrupole, $\alpha^{22}_{mm'}$, polarizability components of fluoromethane. Wormer and Hettema[57] reported dipole−quadrupole and quadrupole polarizabilities of water calculated with the origin of

TABLE 1: Molecular Properties of CH_3F[a]

property	SCF	MP2	MP4	literature
		Multipole Moments		
$Q_{10} = \mu_z$	−0.80	−0.72	−0.71	−0.73,[b] −0.74[c]
Q_{20}	−2.57	−2.31	−2.27	−2.63,[d] −2.42[e]
		Polarizabilities		
α_{00}^{11}	16.47	17.78	17.94	16.52[f]
α_{11}^{11}	15.54	16.50	16.58	15.56[f]
$\bar{\alpha}$	15.85	16.93	17.03	16.79,[c] 16.94[g]
α_{00}^{21}	26.28	29.37		
α_{11}^{21}	1.30	2.86		
α_{21}^{21}	9.08	9.16		
α_{00}^{22}	186.92	206.47	207.56	
α_{11}^{22}	155.54	176.82	178.85	
α_{22}^{22}	106.45	114.44	114.89	
α_{12}^{22}	−14.59	−15.86		

[a] The origin is at the carbon atom with a positive *z*-axis directed along the C−F bond. All values in atomic units. Conversion factors: dipole moment: $ea_0 = 8.478\,356 \times 10^{-30}$ C m; quadrupole moment 1 $ea_0^2 = 4.486\,552 \times 10^{-40}$ C m^2; dipole polarizability $e^2a_0^2E_h^{-1} = 1.648\,78 \times 10^{-41}$ C^2 m^2 J^{-1}; dipole−quadrupole polarizability $e^2a_0^3E_h^{-1} = 8.724\,97 \times 10^{-52}$ C^2 m^3 J^{-1}; quadrupole polarizability $e^2a_0^4E_h^{-1} = 4.617\,05 \times 10^{-62}$ C^2 m^4 J^{-1}. The following relationships hold: $\alpha_{11}^{11} = \alpha_{-1-1}^{11}$; $\alpha_{11}^{21} = \alpha_{-1-1}^{21}$; $\alpha_{21}^{21} = \alpha_{-2-1}^{21}$; $\alpha_{11}^{22} = \alpha_{-1-1}^{22}$; $\alpha_{22}^{22} = \alpha_{-2-2}^{22}$; $\alpha_{12}^{22} = \alpha_{21}^{22} = -\alpha_{-1-2}^{22} = -\alpha_{-2-1}^{22}$. [b] Previously published experimental value.[52] [c] Previouslypublished relaxed MP2 value.[53] [d] SCF value calculated from results of Amos[54] assuming the geometry of CH_3F used in this work. [e] Calculated from previously published MP2 value.[55] [f] Previously published SCF value.[54] [g] Previously published experimental value (linear extrapolation to zero frequency).[53]

TABLE 2: Molecular Properties of H_2O[a]

property	SCF	MP2	MP4	literature
		Multipole Moments		
$Q_{10} = \mu_z$	0.78	0.73	0.72	0.72,[b] 0.73,[c] 0.73[d]
Q_{20}	0.10	0.08	0.08	0.084[e]
Q_{22}	2.13	2.18	2.15	2.21[e]
		Polarizabilities		
α_{00}^{11}	8.49	9.73	9.81	9.93,[f] 9.91[g]
α_{11}^{11}	9.17	10.05	10.15	10.13,[f] 10.31[g]
α_{-1-1}^{11}	7.82	9.53	9.58	9.76,[f] 9.55[g]
$\bar{\alpha}$	8.49	9.77	9.84	9.78,[b] 9.94,[f] 9.64[h]
α_{00}^{21}	3.53	4.40		
α_{11}^{21}	9.13	9.85		
α_{-1-1}^{21}	2.73	3.88		
α_{20}^{21}	2.91	3.01		
α_{00}^{22}	28.11	32.92	33.13	
α_{11}^{22}	47.70	54.08	54.93	
α_{22}^{22}	34.73	41.45	41.74	
α_{-1-1}^{22}	26.57	33.14	33.41	
α_{-2-2}^{22}	30.57	38.12	38.53	
α_{02}^{22}	0.60	2.36		

[a] The origin is at the oxygen atom with the molecule in the *xz* plane, and a negative *z*-axis bisecting the HOH angle. All values are given in atomic units. See Table 1 for conversion factors. The following relationship holds: $\alpha_{02}^{22} = \alpha_{20}^{22}$. [b] Previously published CCSD(T) value.[56] [c] Previously published MP2 value.[57] [d] Previously published experimental value.[58] [e] Calculated using the previously published experimental values of the dipole moment[58] and the components of the quadrupole moment.[59] [f] Previously published MP4 value.[60] [g] Previously published experimental value.[61] [h] Previously published experimental value.[62]

multipole expansion placed at the center of mass of the molecule. Results in Table 2 correspond to the origin placed at the oxygen atom, but for comparison we also calculated these properties at the center of mass. In contrast to dipole polarizabilities, for $\alpha_{mm'}^{21}$ and $\alpha_{mm'}^{22}$ we found larger differences compared to the values of Wormer and Hettema, particularly for α_{-1-1}^{21} and α_{-1-1}^{22} components. The main reason for these differences is the lack of f symmetry functions in our basis set. We verified that adding f symmetry functions to our basis set produced results in better agreement with the values of dipole−quadrupole and quadrupole polarizabilities reported by Wormer and Hettema.

B. Orientations of the Monomers. The radial dependence of the interaction energy was examined for nine configurations which are shown in Figure 1. For configurations for which additional calculations with a basis set that included bond functions were performed, the location of bond functions is denoted by a dot (•). The C-1 structure was chosen to provide the characterization of the linear C−F···H−O hydrogen bond. It has been previously examined by Howard et al.[23] The C-2 and C-3 structures are similar to the most attractive configurations found for the CH_4···H_2O complex.[26] The C-4 and C-5 structures have C−H···O hydrogen bonds and correspond to approaches A and B of the study of the same system by Alkorta and Maluendes,[25] except that their intramolecular geometry for fluoromethane was slightly different ($r_{CH} = 2.079\ a_0$, $r_{CF} = 2.613\ a_0$, ∠HCH = 110°37′).[63] The C-6 structure is related to the previous two although instead of the linear C−H···O hydrogen bond we considered a contact between two hydrogen atoms of fluoromethane and lone pairs of the oxygen atom. The C-7 and C-8 structures were chosen because of the alignment of the dipoles of the two molecules. Finally, the C-9 structure with a bent C−F···H−O hydrogen bond was examined and found to be the global minimum so its radial dependence was considered as well.

The C-1, C-7, C-8, and C-9 orientations are the most stable overall because of the attractive electrostatic and dispersion energies. In fact, these four configurations are more stable than the other five at all investigated levels of theory. Because of the similarities of the radial dependence of the overall interaction energy as well as its components, the nine configurations examined were divided into five groups characterized by the linear C−F···H−O hydrogen bond (C-1), the bent C−F···H−O hydrogen bond (C-9), the alignment of the dipoles (C-7 and C-8), the C−H···O hydrogen bond (C-4, C-5, and C-6), and the repulsive interactions (C-2 and C-3).

In addition to the just mentioned nine configurations for which we performed calculations at different intermolecular separations, we also examined 50 randomly generated structures to take into account the areas of the potential energy surface which the nine configurations did not probe.

C. Interaction Energy and Its Components. The radial dependence of the interaction energy is shown in Table 3, where R_{C-O} denotes the C···O separation and R_{com} denotes the center of mass separation, both in a_0. The most stable configuration presented in Table 3 is the C-9 structure shown in Figure 1. It contains a bent C−F···H−O hydrogen bond with a C···O separation of 6.15 a_0. The F···H distance is equal to 4.0 a_0; the F···H−O angle, a measure of nonlinearity of the hydrogen bond, is equal to 144°; the C−F···O angle is approximately 90°; and the water molecule lies in the plane formed by C, F, and one of the hydrogen atoms of fluoromethane. An interesting feature of this structure is the formation of a secondary C−H···O hydrogen bond with the H···O distance of 4.9 a_0 which is the most probable explanation of its increased stability. The

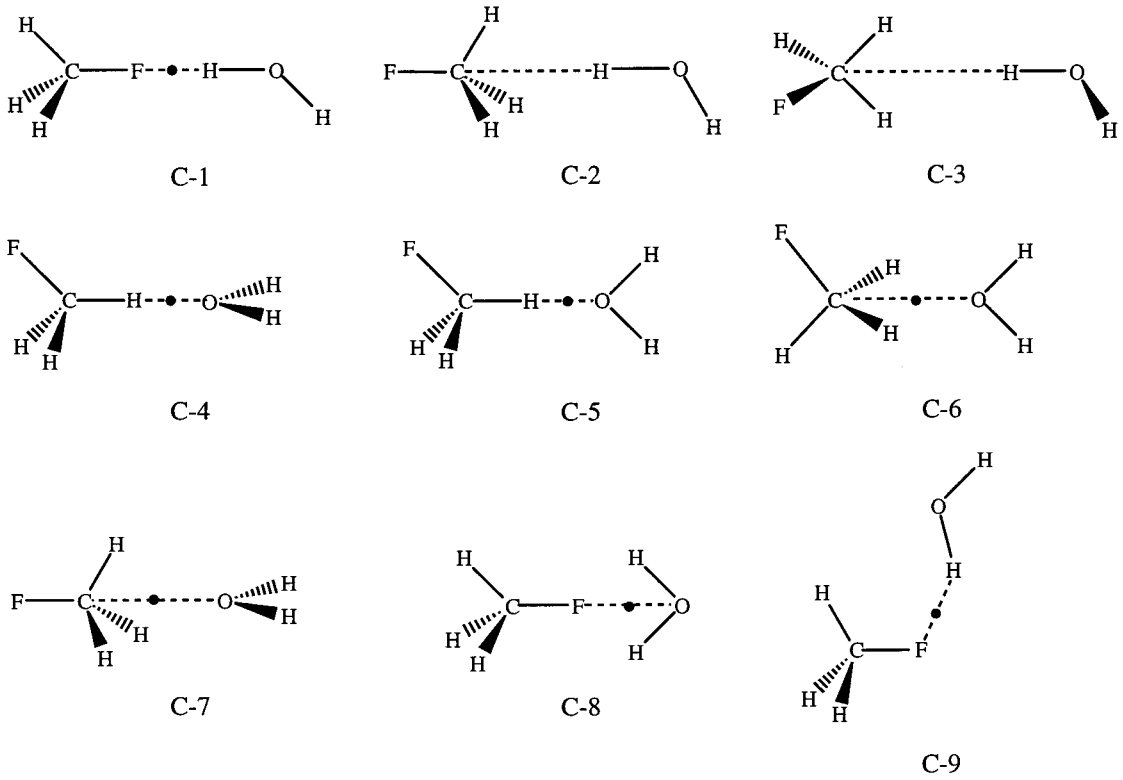

Figure 1. Configurations of the $CH_3F\cdots H_2O$ complex examined in this work. Dots indicate the position of bond functions for the seven attractive configurations.

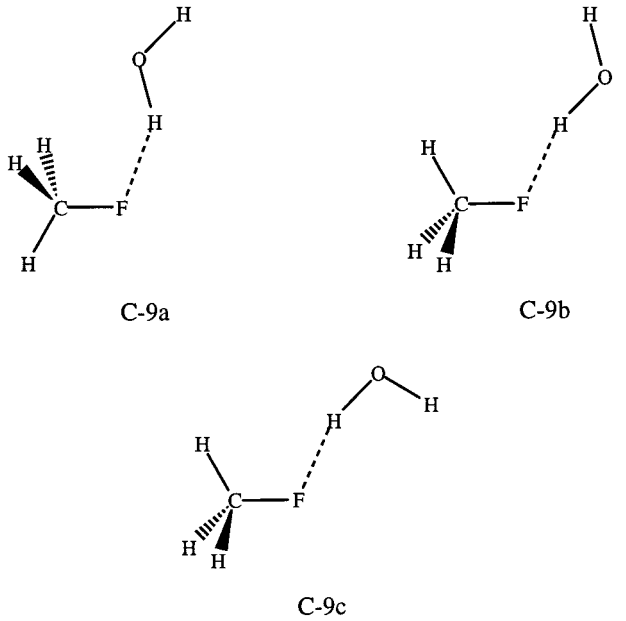

Figure 2. Three modified configurations derived from the C-9 structure of $CH_3F\cdots H_2O$.

interaction energy for this geometry is $-5291\ \mu E_h$ at the MP4 level of theory. The global minimum area contains additional shallower wells corresponding to structures whose interaction energies are within 100 μE_h of the global minimum. For example, the C-9a structure in Figure 2 which results when the fluoromethane molecule is rotated by 60° around its C_3 axis is only 86 μE_h higher in energy than the most stable C-9 structure. On the other hand, if the water molecule is rotated by 180° with respect to the line connecting the two hydrogen atoms, which results in the C-9b structure in Figure 2, the interaction energy is equal to only $-1228\ \mu E_h$. Similarly, the C-9c structure for which the position of the oxygen atom with respect to fluoromethane is the same as in C-9b is much less stable than C-9. However, its interaction energy of $-2278\ \mu E_h$ significantly exceeds the magnitude of the interaction energy for the C-9b structure. This is caused by the stabilizing interaction between fluorine atom and the more remote hydrogen atom of the water molecule. All this shows that the presence of the C−H···O interaction is important in stabilizing the global minimum structure, although the overall interaction energy is not very sensitive to certain geometrical modifications such as the rotation of the fluoromethane molecule around its C_3 axis. The just described differences in the interaction energy for different C-9 structures depicted in Figures 1 and 2 have their origin in changes of the electrostatic component. The differences between other components for the four C-9 structures considered are much smaller.

The geometry of the C−F···H−O hydrogen bond in the C-9 structure shares some similarities with the structures determined by Murray-Rust et al.[4] in their X-ray study of C−F···H−(O, N) hydrogen bonds. They specified geometries of C−F···H−N hydrogen bonds for two systems in which the F···H separations were 4.3 and 4.46 a_0, respectively, and the F···H−N angles were 141° and 155°. These parameters have values similar to the already mentioned F···H distance equal to 4.04 a_0 and the F···H−O angle equal to 144° which were found for the C-9 structure. However, the C−F···H hydrogen bonds described by Murray-Rust et al. involve multiple hydrogen bonds in chelate-like complexes rather than a cyclic arrangement with two hydrogen bonds of different lengths such as in our case. Although good agreement between our geometrical parameters is likely to be accidental, our conclusions agree with those of Murray-Rust et al. who stated that "C−F can act as a weak proton acceptor" and that "C−F···H−O bonds are energetically favorable, but that other stronger interactions are usually formed in preference."

TABLE 3: Interaction Energy and Its Components Calculated Using Sadlej's Basis Set for the Nine Configurations of $CH_3F\cdots H_2O$[a]

R_{C-O}	R_{com}	$\epsilon_{es}^{(10)}$	ϵ_{exch}^{HL}	ΔE_{def}^{SCF}	$\epsilon_{disp}^{(20)}$	ΔE^{MP2}	ΔE^{MP4}
			Configuration C-1				
7.00	5.525	−21 989.7	58 389.4	−15 861.0	−10 033.8	18 268.5	18 697.3
8.00	6.525	−6 916.3	7 048.0	−2 141.5	−2 793.6	−2 763.7	−2 791.4
8.50	7.025	−4 647.3	2 410.9	−913.6	−1 550.1	−3 522.5	−3 560.8
9.00	7.525	−3 406.3	819.0	−434.7	−893.2	−3 171.3	−3 192.4
10.00	8.525	−2 099.1	92.6	−133.6	−334.9	−2 100.8	−2 092.2
12.00	10.525	−997.6	1.0	−26.3	−71.9	−940.1	−921.1
			Configuration C-2				
6.00	7.325	2 072.2	5 029.1	−1 375.0	−2 909.4	3 199.0	2 951.6
7.00	8.324	1 814.8	666.6	−304.4	−1 014.8	1 045.5	878.3
8.00	9.324	1 290.4	82.9	−99.5	−405.0	717.0	622.5
9.00	10.324	922.3	9.3	−42.8	−182.6	584.9	530.1
10.00	11.324	680.5	0.8	−21.4	−91.0	476.5	442.2
12.00	13.324	402.0	−0.1	−6.8	−28.2	311.5	294.9
			Configuration C-3				
6.00	6.508	−833.5	10 204.5	−2 430.3	−3 865.7	3 992.8	3 774.1
7.00	7.490	897.6	1 534.4	−505.3	−1 315.5	669.7	498.5
8.00	8.476	855.3	218.6	−141.7	−504.3	351.9	255.9
9.00	9.465	632.6	29.5	−53.4	−219.5	314.6	262.6
10.00	10.456	457.0	3.6	−24.5	−106.5	272.1	242.2
12.00	12.441	252.1	0.0	−7.0	−31.9	180.2	167.9
			Configuration C-4				
6.00	6.703	−6 683.7	10 328.6	−2 148.6	−3 396.5	−18.9	−50.5
6.50	7.194	−3 807.6	3 998.8	−965.4	−1 915.6	−1 666.9	−1 719.6
7.00	7.686	−2 440.4	1 533.3	−475.8	−1 115.9	−1 908.5	−1 951.5
7.50	8.179	−1 722.2	582.7	−256.9	−674.0	−1 704.0	−1 731.4
8.00	8.672	−1 300.3	219.6	−150.4	−422.2	−1 407.2	−1 421.2
9.00	9.662	−833.6	30.5	−62.1	−182.8	−911.2	−909.7
10.00	10.653	−580.2	4.1	−30.0	−88.5	−604.3	−597.5
12.00	12.640	−317.6	0.0	−9.1	−26.7	−304.8	−297.7
			Configuration C-5				
6.00	6.703	−6 837.9	10 343.6	−2 150.9	−3 398.3	−148.5	−178.0
6.50	7.194	−3 933.9	4 004.3	−967.0	−1 916.2	−1 780.9	−1 831.3
7.00	7.686	−2 543.0	1 535.4	−476.9	−1 116.0	−2 003.5	−2 044.3
7.50	8.179	−1 805.4	583.5	−257.5	−674.0	−1 782.0	−1 807.4
8.00	8.672	−1 367.9	219.9	−150.8	−422.2	−1 470.9	−1 483.2
9.00	9.662	−878.5	30.5	−62.3	−182.8	−953.9	−951.2
10.00	10.653	−610.6	4.1	−30.2	−88.5	−633.3	−625.6
12.00	12.640	−332.4	0.0	−9.2	−26.7	−318.9	−311.4
			Configuration C-6				
6.00	6.703	−2 840.5	3 300.7	−560.6	−1 948.5	−1 178.8	−1 300.6
6.50	7.194	−1 905.8	1 264.8	−310.7	−1 159.2	−1 617.0	−1 698.0
7.00	7.686	−1 415.0	479.7	−186.0	−713.1	−1 529.5	−1 579.7
7.50	8.178	−1 117.8	180.2	−118.1	−453.7	−1 302.6	−1 331.5
8.00	6.672	−915.2	67.0	−78.5	−298.0	−1 071.8	−1 086.7
9.00	9.662	−648.7	9.1	−38.2	−139.7	−718.5	−719.2
10.00	10.653	−478.7	1.1	−20.3	−71.9	−498.1	−493.9
12.00	12.640	−279.8	0.0	−6.9	−23.3	−268.1	−262.7
			Configuration C-7				
5.00	6.524	−7 048.7	11 089.4	−1 593.8	−4 468.3	283.6	155.2
5.50	7.024	−4 230.8	4 130.6	−740.4	−2 545.8	−2 132.7	−2 245.4
6.00	7.524	−2 921.6	1 518.5	−388.9	−1 497.4	−2 555.3	−2 635.2
6.50	8.024	−2 225.3	551.2	−225.7	−911.1	−2 337.1	−2 386.0
7.00	8.524	−1 797.5	197.5	−141.2	−573.0	−1 976.8	−2 001.9
8.00	9.524	−1 277.9	24.5	−64.1	−248.2	−1 354.3	−1 352.9
9.00	10.524	−958.1	2.9	−32.9	−119.5	−954.3	−943.4
10.00	11.524	−739.7	0.3	−18.2	−62.8	−702.9	−689.8
12.00	13.524	−467.4	0.0	−6.5	−20.9	−421.1	−409.9
			Configuration C-8				
7.00	5.476	−16 116.7	32 204.9	−4 035.3	−7 163.2	9 893.7	9 636.4
8.00	6.476	−5 150.5	4 165.3	−760.4	−2 134.6	−2 342.5	−2 486.2
8.50	6.976	−3 626.7	1 484.7	−386.1	−1 218.0	−2 800.5	−2 882.0
9.00	7.476	−2 795.1	527.7	−217.4	−720.3	−2 569.0	−2 607.5
10.00	8.476	−1 892.3	65.9	−87.4	−283.2	−1 835.8	−1 831.4
12.00	10.476	−1 034.1	0.9	−22.6	−64.7	−941.2	−921.2
			Configuration C-9				
5.00	4.573	−27 555.2	53 434.9	−12 328.3	−11 796.0	8 800.0	9 275.5
5.50	5.059	−14 732.2	20 004.9	−4 762.2	−6 458.7	−2 475.6	−2 359.4
6.15	5.743	−7 581.9	5 371.1	−1 390.8	−3 042.8	−5 277.1	−5 290.7
6.50	6.037	−5 677.2	2 608.8	−857.9	−2 067.6	−4 998.2	−5 020.0
7.00	6.529	−4 001.5	916.5	−409.7	−1 225.2	−4 111.3	−4 124.2
8.00	7.515	−2 298.0	108.4	−119.8	−480.5	−2 492.1	−2 483.0
10.00	9.497	−993.2	1.2	−20.5	−106.3	−992.0	−974.3
12.00	11.485	−513.5	−0.1	−5.6	−32.5	−483.5	−471.0

[a] The MP4 results were calculated using the frozen core approximation, and the MP2 results were obtained by taking into account the correlation of all electrons. R_{C-O} and R_{com} are given in a_0 and energies in μE_h.

The C-1 structure which contains a linear C−F···H−O hydrogen bond is much higher in energy than the C-9 configuration. The interaction energy at the radial minimum with the C···O distance of 8.5 a_0 was found to be only −3561 μE_h. It is this value that should be considered as the true measure of the intrinsic strength of the C−F···H−O hydrogen bond since in the C-1 configuration there are no additional hydrogen bonds which could further stabilize the structure. The C-8 structure, which lacks a linear hydrogen bond, but in which the dipoles of the two molecules are aligned, is the third most stable configuration, possessing the MP4 interaction energy of −2882 μE_h at a C···O separation of 8.5 a_0. Slightly less stable is the C-7 configuration with $\Delta E^{MP4} = -2635$ μE_h. The C−H···O hydrogen bonded structures C-4, C-5, and C-6 have interaction energies of only −2044, −1952, and −1698 μE_h, respectively, at the MP4 level of theory. In contrast to the $CH_4\cdots H_2O$ complex[26] for which the C-2 and C-3 configurations were found to be the most attractive, in the present case they were found to be repulsive at the MP4 level of theory for all distances examined.

To gain some insight into the nature of the interaction between CH_3F and H_2O, the electrostatic, exchange, deformation, and dispersion energies were examined for all nine configurations as functions of the center of mass separation of the two interacting molecules. The use of the center of mass separations in Figures 3−7 rather than the C···O separations was dictated by the fact that the former emphasized qualitative similarities between energy components for different configurations. This allowed us to show plots for only one chosen configuration from each of the five groups described earlier. For example, the curves representing the electrostatic energy, $\epsilon_{es}^{(10)}$, as a function of R_{com} are very similar for the C-1, C-4, C-5, C-6, C-7, and C-8 structures and therefore in Figure 3 the curves for three of them, C-5, C-6, and C-8, are omitted.

As anticipated, the electrostatic energy plays a large role, significantly more so than for $CH_4\cdots H_2O$.[26] Interestingly, the dipole−dipole interaction does not explain the electrostatic trend well: the C-7 and C-8 configurations, which have molecular dipoles aligned, are considerably less attractive electrostatically at their most attractive intermolecular separations than the C-1 and C-9 configurations, which do not represent the alignment of dipoles. Higher order moments, whose interactions with the dipole moments and each other are more favorable for C-1 or C-9 than for C-7 or C-8 structures, account for these results. The influence of higher order moments is also responsible for the differences between the electrostatic energies of the two

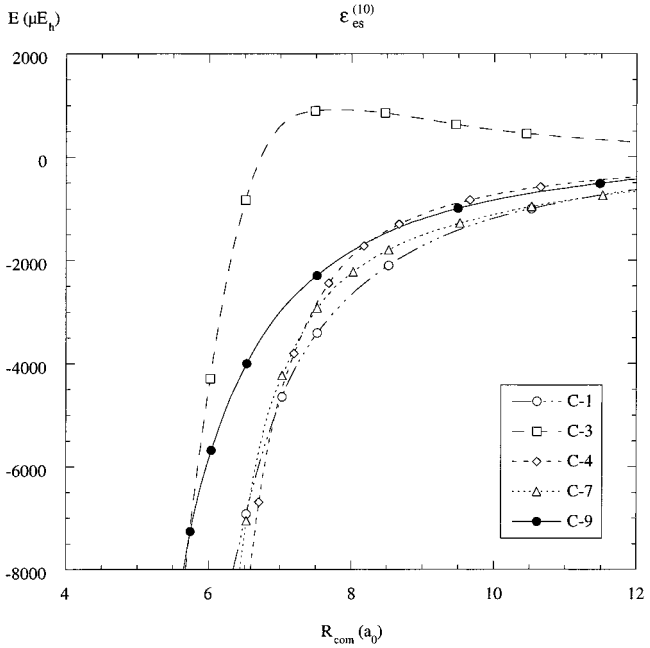

Figure 3. Radial dependence of the electrostatic energy, $\epsilon_{es}^{(10)}$, for selected configurations.

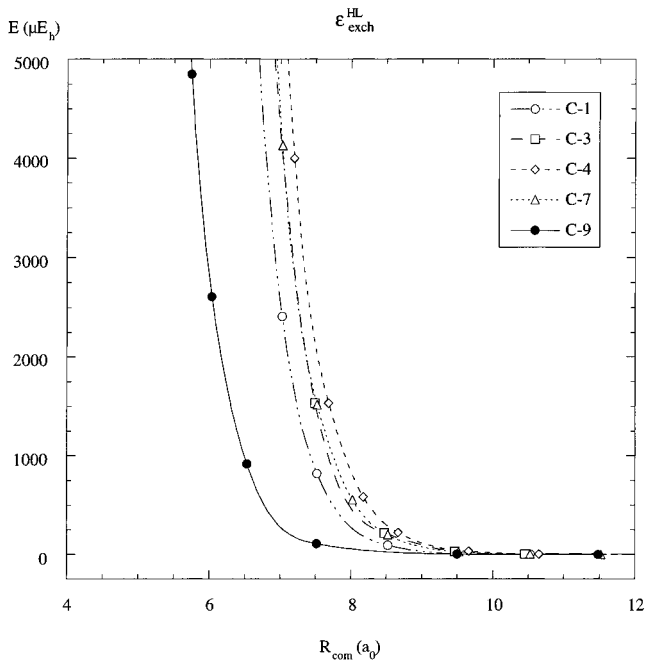

Figure 4. Radial dependence of the exchange energy, ϵ_{exch}^{HL}, for selected configurations.

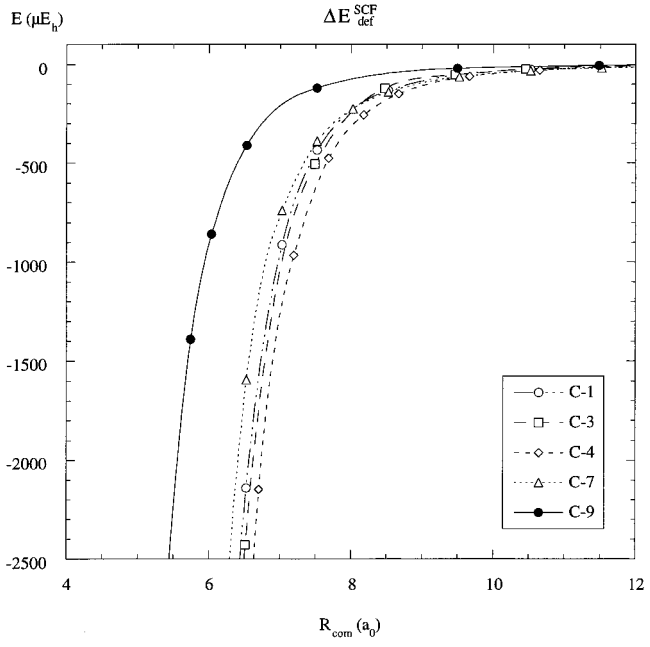

Figure 5. Radial dependence of the SCF-deformation energy, ΔE_{def}^{SCF}, for selected configurations.

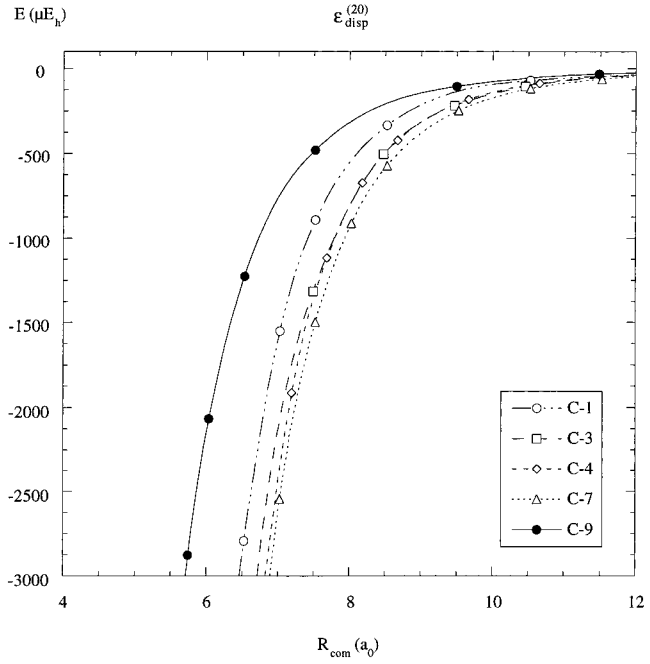

Figure 6. Radial dependence of the dispersion energy, $\epsilon_{disp}^{(20)}$, for selected configurations.

repulsive configurations, C-2 and C-3, at the center of mass separations shorter than 6.7 a_0, where the former remains repulsive and the latter becomes attractive as shown in Figure 3. The electrostatic energy calculated from a multipole expansion does not account for a significant portion of the nonexpanded energy, so it appears that penetration effects are important.

The second-order intramolecular correlation correction to the electrostatic energy, $\epsilon_{es,r}^{(12)}$, displays a markedly different trend than that of $\epsilon_{es}^{(10)}$. The C-1, C-8, and C-9 configurations have repulsive $\epsilon_{es,r}^{(12)}$ values at their most attractive geometries. On the other hand, C-2 and C-3 have attractive $\epsilon_{es,r}^{(12)}$ values at all distances studied. The remaining configurations have values close to each other and are scattered between these two extremes. The $\epsilon_{es,r}^{(12)}$ component is not very important compared to $\epsilon_{es}^{(10)}$ since its magnitude for most structures is smaller than 10% of $\epsilon_{es}^{(10)}$. Only for the C-1 configuration does it amount to approximately 13%.

The exchange energy, ϵ_{exch}^{HL}, shown in Figure 4 is much less repulsive at short intermolecular separations for the C-9 structure than for any other configuration. This is due to the bent geometry of the C-9 structure in which the centers of mass of the two molecules must be closer to each other before the repulsive forces reach the same level of magnitude as in other configurations. The radial dependence of the exchange energy for the remaining eight structures is fairly similar. This is shown in Figure 4 for four of the eight configurations.

TABLE 4: Interaction Energy and Its Components at the Radial Minima for Each of the Seven Attractive Configurations of $CH_3F\cdots H_2O$ Studied[a]

configuration	basis set	$\epsilon_{es}^{(10)}$	ϵ_{exch}^{HL}	ΔE_{def}^{SCF}	$\epsilon_{disp}^{(20)}$	ΔE^{MP2}	ΔE^{MP4}
C-1 (8.50)	S	−4647.3	2410.9	−913.6	−1550.1	−3522.5	−3560.8
	S+bf	−4730.0	2409.6	−938.7	−1716.4	−3851.0	−3919.9
C-4 (7.00)	S	−2440.4	1533.3	−475.8	−1115.9	−1908.5	−1951.5
	S+bf	−2433.3	1528.8	−484.3	−1264.7	−2064.6	−2131.7
C-5 (7.00)	S	−2543.0	1535.4	−476.9	−1116.0	−2003.5	−2044.3
	S+bf	−2534.9	1529.9	−485.5	−1264.9	−2162.1	−2228.1
C-6 (6.50)	S	−1905.8	1264.8	−310.7	−1159.2	−1617.0	−1698.0
	S+bf	−1892.6	1261.7	−321.7	−1332.1	−1748.2	−1859.2
C-7 (6.00)	S	−2921.6	1518.5	−388.9	−1497.4	−2555.3	−2635.2
	S+bf	−2864.0	1513.9	−403.8	−1736.8	−2736.1	−2854.8
C-8 (8.50)	S	−3626.7	1484.7	−386.1	−1218.0	−2800.5	−2882.0
	S+bf	−3641.7	1492.9	−398.0	−1385.5	−2946.4	−3064.2
C-9 (6.15)	S	−7581.9	5371.1	−1390.8	−3042.8	−5277.1	−5290.7
	S+bf	−7537.7	5366.9	−1552.8	−3373.5	−5648.6	−5739.1

[a] The C···O separation in a_0 is given in parentheses. S and S+bf denote, respectively, Sadlej's basis set without and with an additional set of bond functions located as shown in Figure 1. The MP4 results were calculated using the frozen core approximation, and the MP2 results were obtained by taking into account the correlation of all electrons. Energies are given in μE_h.

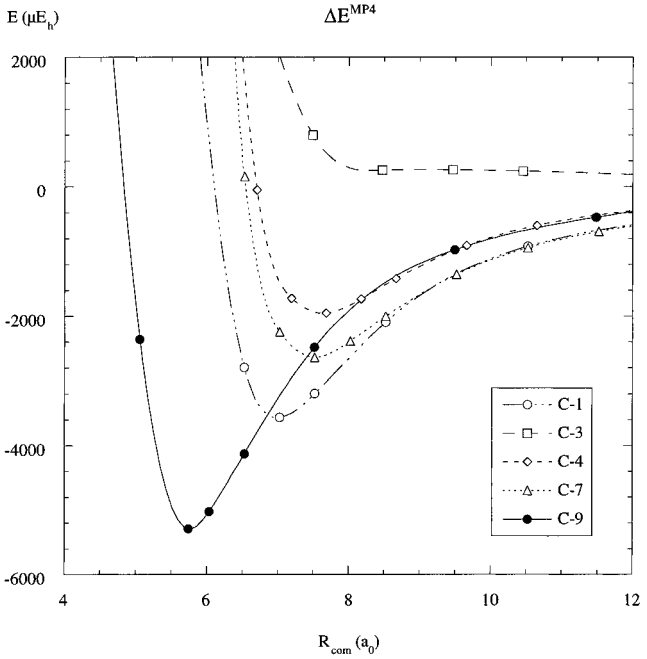

Figure 7. Radial dependence of the MP4 interaction energy, ΔE^{MP4}, for selected configurations.

The SCF deformation energy presented in Figure 5 amounts to less than one-quarter of the electrostatic energy at each of the radial minima for the seven attractive configurations. As with the exchange energy, the curve representing ΔE_{def}^{SCF} for the C-9 configuration is shifted to shorter intermolecular separations in comparison to the curves for the remaining configurations which are fairly close together. The second-order induction energy, $\epsilon_{ind,r}^{(20)}$, mirrors the trends of the deformation energy although at short intermolecular distances the former is much more attractive due to the neglect of exchange effects.

The dispersion energy shown in Figure 6 is generally less important than the electrostatic energy, in contrast to the large role of the former in the $CH_4\cdots H_2O$ system. At the radial minima, $\epsilon_{disp}^{(20)}$ is by far the most attractive for the C-9 configuration and, as with other components, the curve representing its dispersion energy is shifted to shorter intermolecular separations. The similarities between the curves for the remaining structures are apparent in Figure 6. The dispersion energy is consistently the most attractive of the five components examined for the repulsive C-2 and C-3 configurations.

The MP4 interaction energy, ΔE^{MP4}, is plotted in Figure 7. From the results of the component studies above, it is clear that a highly attractive electrostatic term, $\epsilon_{es}^{(10)}$, and a significant contribution from the dispersion energy, $\epsilon_{disp}^{(20)}$, are responsible for the increased stability of the C-9 configuration. The differences between component energies for the C-1, C-4 and C-7 structures are much smaller in magnitude, but the curves representing ΔE^{MP4} are clearly different. This underscores the fact that even small modifications of component energies can have a profound effect on the supermolecule interaction energy.

In general, the MP2 interaction energies calculated in this work qualitatively resemble the MP4 results. That is, the shapes of the ΔE^{MP2} and ΔE^{MP4} curves and the locations of attractive wells are similar. However, for the seven attractive structures ΔE^{MP2} often significantly underestimates the interaction energy at short distances, with the difference reaching 476 μE_h, or 5%, for the C-9 structure at $R_{C-O} = 5.0\ a_0$. The underestimation is somewhat smaller in magnitude, but often larger percentagewise, at the radial minimum of each configuration (by up to 80 μE_h, or 5%, at $R_{C-O} = 6.5\ a_0$ for C-6). For R_{C-O} between 1 and 2 a_0 larger than the radial minimum, ΔE^{MP2} often crosses ΔE^{MP4} and becomes more attractive at long distances. For the two completely repulsive configurations, ΔE^{MP2} is more repulsive than ΔE^{MP4} at all distances studied. Furthermore, relative differences are large, reaching 38% for the C-3 structure at 8.0 a_0, mainly because interaction energies are small in magnitude. Interestingly, for the global minimum, ΔE^{MP2} and ΔE^{MP4} are very close to each other with a difference of only −13.6 μE_h.

D. Effect of Bond Functions. The calculations for the radial minima for each of the seven attractive configurations were also performed using a basis set that included bond functions located as shown in Figure 1. The results of these calculations are compared in Table 4 with the results of calculations in which a basis set without bond functions was used. By adding bond functions, the MP4 interaction energy is lowered in every case. The most significant changes are 448 μE_h (8%) for the C-9 structure and 359 μE_h (9%) for the C-1 structure. The dispersion energy, $\epsilon_{disp}^{(20)}$, is typically the most affected component, becoming 10−14% more attractive when bond functions are used. This is yet another confirmation of the known effect[51] of bond functions on the saturation of dispersion energy. In the present case, this effect is quite pronounced since Sadlej's basis sets lack orbitals with symmetry higher than d. Other energy components are not significantly affected by the addition of bond functions. For example, the electrostatic energy changes by 2%

or less and the exchange energy by less than 0.6%. The unusually large difference of 10.4% was observed for the SCF deformation energy but only for the C-9 structure.

IV. Potential Energy Surface

A potential energy surface for the $CH_3F\cdots H_2O$ interaction has been developed using a similar functional form to the one proposed for the water dimer by Wheatley.[64] Wheatley's method uses components of the interaction energy so that fewer points on the potential energy surface need to be fitted in order to obtain a reasonable description of the potential energy surface.

First, the properties of the monomers were calculated, as described earlier. Next, the SCF and MP2 multipole moments and polarizabilities were used to attempt to reproduce the electrostatic and induction energies for all configurations in Table 3 and additional 50 random structures.

The interaction energy was divided into five contributions:

$$E = E_{\mathrm{es}} + E_{\mathrm{ind}} + E_{\mathrm{disp}} + E_{\mathrm{rep}} + E_{\mathrm{corr}} \tag{5}$$

The multipole-expanded electrostatic, E_{es}, was calculated using the distributed multipole moments Q_{lm}:

$$E_{\mathrm{es}} = \sum_{ab}\sum_{lm,l'm'} Q_{lm,a}Q_{l'm',b}T_{lm,l'm'}(R_{ab},\Omega_{ab}) \tag{6}$$

where l and m are the usual labels used for spherical harmonics, $T_{lm,l'm'}$ is a function of the nuclear separation R_{ab} and the relative monomer orientations Ω_{ab}. The summation over l and l' was performed up to $l + l' = 4$, since interactions of higher ranks are expected to contribute little to the potential.[64] Good agreement between the multipole representation of the electrostatic energy and the nonexpanded $\epsilon_{\mathrm{es}}^{(10)}$ component was found only for long intermolecular distances. As the intermolecular distances decrease, the differences between $\epsilon_{\mathrm{es}}^{(10)}$ and E_{es} increase due to penetration effects.

The induction energy was calculated using the equation

$$E_{\mathrm{ind}} = -\frac{1}{2}\sum_{\mathrm{A}}\sum_{lm,l'm'} \alpha_{mm'}^{ll'}F_{lm}^{\mathrm{A}}F_{l'm'}^{\mathrm{A}} \tag{7}$$

where $\alpha_{mm'}^{ll'}$ denotes a polarizability of appropriate rank and F_{lm}^{A} denotes an electric field induced by molecule B on molecule A:

$$F_{lm}^{\mathrm{A}} = \sum_{b,l'',m''} Q_{l''m'',b}T_{lm,l''m''}(R_{ab},\Omega_{ab}) \tag{8}$$

In eq 8, Q denotes a multipole moment, and **T** an interaction tensor. As with the electrostatic energy, using eq 7, we were able to reproduce the $\epsilon_{\mathrm{ind,r}}^{(20)}$ component only for long distances.

The exchange repulsion energy was calculated using the formula

$$E_{\mathrm{rep}} = \sum_{ab}\exp(-\alpha_{ab}R_{ab})\sum_{lm,l'm'} A_{lm,l'm'}^{ab}S_{l,l',l+l'}^{m,m'}(\Omega_{ab}) \tag{9}$$

where α and A are adjustable parameters determined by fitting the Heitler−London exchange energy, $\epsilon_{\mathrm{exch}}^{\mathrm{HL}}$, and the **S** tensor is determined by the orientation[65]

$$S_{l,l',l''}^{m,m'} = i^{l-l'-l''}\sum_{k,k',k''}\begin{pmatrix} l & l' & l'' \\ k & k' & k'' \end{pmatrix} D_{km}^{l}(\omega_a)^*D_{k'm'}^{l'}(\omega_b)^*D_{k''0}^{l''}(\omega)^* \tag{10}$$

Here, ω_a and ω_b denote the local axis orientations of sites a and b relative to a fixed set of axes, and ω denotes the orientation of the vector from site a to site b relative to the same fixed axes. D's denote the Wigner rotation matrices, whereas the parenthetical rows of coefficients represent a Wigner 3-j symbol.[66] Overall, 24 adjustable parameters were used. To ensure that the fit of the exchange repulsion energy was not unphysical, we had to include in the fit the results of some selected configurations at short intermolecular separations.

Calculation of the dispersion energy was achieved using

$$E_{\mathrm{disp}}(R_{ab},\Omega_{ab}) = \left[\sum_{n=6}^{8} C_n(\Omega_{ab})R^{-n}\right]G(R_{ab}) \tag{11}$$

where

$$C_n(\Omega_{ab}) = \sum_{l,l',l'',m,m'} C_{n;l,l',l''}^{m,m'}S_{l,l',l''}^{m,m'}(\Omega_{ab}) \tag{12}$$

where $C_{n;l,l',l''}^{m,m'}$ are adjustable parameters fitted to $\epsilon_{\mathrm{disp}}^{(20)}$. We used 29 adjustable parameters to describe the dispersion energy. The damping function G suppresses the singularities of the R^{-n} terms in eq 11. It is defined by

$$G(R_{ab}) = \begin{cases} \exp\left[-0.4\left(\dfrac{R_0}{R_{ab}} - 1\right)^2\right] & R_{\mathrm{ab}} < R_0 \\ 1 & R_{ab} \geq R_0 \end{cases} \tag{13}$$

R_0 for the dispersion energy was set as 7.7 a_0 and was chosen from several other values since it gave the fit of the best quality.

The last component which is named "the correlation energy" was fitted to the difference between the MP4 interaction energy and the sum of the already described four components:

$$E_{\mathrm{corr}} = \Delta E^{\mathrm{MP4}} - E_{\mathrm{es}} - E_{\mathrm{ind}} - E_{\mathrm{disp}} - E_{\mathrm{rep}} \tag{14}$$

Its functional form is essentially the same as that of the repulsion energy, but in this case also a corrector-damping function G was applied:

$$E_{\mathrm{corr}} = \sum_{ab}G(R_{ab})\exp(-\beta_{ab}R_{ab})\sum_{lm,l'm'} B_{lm,l'm'}^{ab}S_{l,l',l+l'}^{m,m'}(\Omega_{ab}) \tag{15}$$

where $G(R_{ab})$ is defined by eq 13 with $R_0 = 10.0$ a_0 and is chosen to provide the best fit as in the case of the dispersion energy. β and B are analogous to α and A in eq 9 so in this case also 24 parameters were used. Because of the flexibility of the function given by eq 15 some of the points had to be excluded from the fit. The tests performed on final form of the potential did not show any unphysical behavior for R_{com} larger than 5.0 a_0. For a set of 40 randomly selected structures which were not used in the fit, we found that the fitted potential gave a standard deviation of 342 μE_{h}. A FORTRAN program for evaluating the interaction energy between CH_3F and H_2O is available on request.

V. Summary

The global minimum has been found for the C-9 structure with a bent C−F···H−O hydrogen bond with the C···O separation of 6.15 a_0 and with the MP4 interaction energy of −5739 μE_{h}. The stability of this structure is enhanced by the presence of an additional elongated C−H···O hydrogen bond. The magnitude of this effect does not seem to have been previously examined in the literature although a structure very

similar to C-9 has been found by Caminati et al.[22] for the difluoromethane···water complex. A structure with a linear C−F···H−O hydrogen bond is significantly less stable with the MP4 interaction energy of $-3920\ \mu E_h$ at the C···O separation of 8.0 a_0. Howard et al.[23] have found for a similar configuration a slightly weaker interaction energy of $-3790\ \mu E_h$. They did not provide all of the geometrical parameters used in their calculations, but the equilibrium F···H separation of 3.6 a_0 is significantly shorter from the value of 4.1 a_0 which we found. In their analysis of crystallographic databases, Howard et al.[23] focused on the length of the F···H hydrogen bonds in assessing the propensity of fluorine to act as a hydrogen bond acceptor, but as our calculations show, the stability of the C−F···H−O hydrogen bonds can be greatly influenced by neighboring atoms.

The strength of the C−F···H−O hydrogen bond can be compared to the strength of hydrogen bonds in other complexes. A convenient reference system is the water dimer for which the most accurate estimate of the binding energy appears to have been reported by Klopper et al.[67] Their CCSD(T) result is $8000 \pm 80\ \mu E_h$ (5.02 ± 0.05 kcal/mol). Since we did not use CCSD-(T) theory in the present work, a more appropriate comparison is with the MP2 results obtained by Klopper et al. ($\Delta E^{MP2} = -7896\ \mu E_h$) and Schütz et al.[68] ($\Delta E^{MP2} = -7872\ \mu E_h$). Using the geometry of Klopper et al. and Sadlej's basis set without bond functions, we obtained for the water dimer $\Delta E^{MP2} = -7033\ \mu E_h$. When bond functions were used, the MP2 interaction energy was found to be $-7609\ \mu E_h$ which is 3.6% higher in energy than that the result of Klopper et al. and 3.3% higher than the result of Schütz et al. Good agreement with the literature data for the water dimer validates our approach to the fluoromethane-water system, particularly the results obtained with a basis set that included bond functions. The results for $(H_2O)_2$ can be compared with the interaction energies for the C-9 ($\Delta E^{MP2} = -5649\ \mu E_h$) and C-1 ($\Delta E^{MP2} = -3851\ \mu E_h$) configurations of the $CH_3F\cdots H_2O$ complex obtained with Sadlej's basis set augmented with bond functions. The interaction energy for the C-9 structure amounts to approximately 70% of the results for the water dimer. The interaction energy for the C-1 structure, which in our opinion is a better measure of the intrinsic strength of the C−F···H−O hydrogen bond, is approximately two times smaller than in the water dimer.

From these results, it seems quite possible that a C−F···H−O hydrogen bond interaction in fluorocitrate ester crystals is energetically favorable. Similarly, energetics may be a factor in the difluorotoluene nucleoside's ability to code for adenine. While steric factors are certainly important in these two systems, fluorine's ability to form a hydrogen bond is not insignificant either. Perhaps further studies could determine why the NMR spectrum of 2-fluoroethanol does not show evidence of hydrogen bonding.

Acknowledgment. We acknowledge the support of the National Science Foundation (Grant No. CHE-9616683).

References and Notes

(1) Jeffrey, G. A.; Saenger, W. *Hydrogen Bonding in Biological Structures*; Springer-Verlag: New York, 1991.
(2) Marais, J. S. C. *Ondertepoort J. Vet. Sci.* **1944**, *20*, 67.
(3) Peters, R. A. *Endeavor* **1954**, *90*, 147.
(4) Murray-Rust, P.; Stallings, W. C.; Monti, C. T.; Preston, R. K.; Glusker, J. P. *J. Am. Chem. Soc.* **1983**, *105*, 3206.
(5) Hobza, P.; Mulder, F.; Sandorfy, C. *J. Am. Chem. Soc.* **1981**, *103*, 1360.
(6) Curtiss, L. A.; Frurip, D. J.; Blander, M. *J. Am. Chem. Soc.* **1978**, *100*, 79.
(7) Hagen, K.; Hedberg, K. *J. Am. Chem. Soc.* **1973**, *95*, 8263.
(8) Krueger, P. J.; Mettee, H. D. *Can. J. Chem.* **1964**, *42*, 326.
(9) Barnett, J. E. G. *Carbon−Fluorine Compounds: Chemistry, Biochemistry and Biological Activities*; Elsevier: Amsterdam, 1972.
(10) Krueger, P. J.; Mettee, H. D. *Can. J. Chem.* **1968**, *46*, 2917.
(11) Wyn-Jones, E.; Orville-Thomas, W. *J. Mol. Struct.* **1967**, *1*, 79.
(12) Buckley, P.; Giguere, P. A.; Yamamoto, D. *Can. J. Chem.* **1968**, *46*, 2917.
(13) Almennirgen, A.; Bastiansen, O.; Fernholt, L.; Hedberg, K. *Acta Chem. Scand.* **1971**, *25*, 1946.
(14) Pachler, K. G. R.; Wessels, P. L. *J. Mol. Struct.* **1970**, *6*, 471.
(15) Buckton, K. S.; Azrak, R. G. *J. Chem. Phys.* **1970**, *52*, 5652.
(16) Griffith, R. C.; Roberts, J. D. *Tetrahedron Lett.* **1974**, 3499.
(17) Moran, S.; Ren, R. X.-F.; Rumney, S.; Kool, E. T. *J. Am. Chem. Soc.* **1997**, *119*, 2056.
(18) Ren, R. X.-F.; Chaudhuri, N. C.; Paris, P. L.; Rumney, S.; Kool, E. T. *J. Am. Chem. Soc.* **1996**, *118*, 7671.
(19) Schwitzer, B. A.; Kool, E. T. *J. Am. Chem. Soc.* **1995**, *117*, 1863.
(20) Ryjáček, F.; Kratochvíl, M.; Hobza, P. *Chem. Phys. Lett.* **1999**, *313*, 393.
(21) Tarakeshwar, P.; Kim, K. S.; Brutschy, B. *J. Chem. Phys.* **1999**, *110*, 8501.
(22) Caminati, W.; Melandri, S.; Rossi, I.; Favero, P. G. *J. Am. Chem. Soc.* **1999**, *121*, 10098.
(23) Howard, J. A. K.; Hoy, V. J.; O'Hagan, D.; Smith, G. T. *Tetrahedron* **1996**, *52*, 12613.
(24) Veenstra, D. L.; Ferguson, D. M.; Kollman, P. A. *J. Comput. Chem.* **1992**, *13*, 971.
(25) Alkorta, I.; Maluendes, S. *J. Phys. Chem.* **1995**, *99*, 6457.
(26) Szczęśniak, M. M.; Chałasiński, G.; Cybulski, S. M.; Cieplak, P. *J. Chem. Phys.* **1993**, *98*, 3078.
(27) Suenram, R. D.; Fraser, G. T.; Lovas, F. J.; Kawashima, Y. *J. Chem. Phys.* **1994**, *101*, 7230.
(28) Rybak, S.; Jeziorski, B.; Szalewicz, K. *J. Chem. Phys.* **1991**, *95*, 6576.
(29) Chałasiński, G.; Szczęśniak, M. M. *Mol. Phys.* **1988**, *63*, 205.
(30) Chałasiński, G.; Szczęśniak, M. M.; Cybulski, S. M. *J. Chem. Phys.* **1990**, *92*, 2481.
(31) Cybulski, S. M.; Chałasiński, G.; Moszyński, R. *J. Chem. Phys.* **1990**, *92*, 4357.
(32) Chałasiński, G.; Szczęśniak, M. M. *Chem. Rev.* **1994**, *94*, 1723.
(33) Cybulski, S. M. *J. Chem. Phys.* **1992**, *97*, 7545.
(34) Gutowski, M.; van Duijneveldt, F. B.; Chałasiński, G.; Piela, L. *Chem. Phys. Lett.* **1986**, *129*, 325.
(35) Gutowski, M.; van Lenthe, J. H.; Verbeek, J.; van Duijneveldt, F. B.; Chałasiński, G. *Chem. Phys. Lett.* **1986**, *124*, 370.
(36) van Lenthe, J. H.; van Duijneveldt-van de Rijdt, J. G. C. M.; van Duijneveldt, F. B. *Adv. Chem. Phys.* **1987**, *69*, 521.
(37) Chałasiński, G.; Gutowski, M. *Chem. Rev.* **1988**, *88*, 943.
(38) Szczęśniak, M. M.; Scheiner, S. *J. Chem. Phys.* **1986**, *84*, 6328.
(39) Boys, S. F.; Bernardi, F. *Mol. Phys.* **1970**, *19*, 553.
(40) Duncan, J. L. *J. Mol. Struct.* **1970**, *6*, 447.
(41) Benedict, W. S.; Gailar, N.; Plyler, E. K. *J. Chem. Phys.* **1956**, *24*, 1139.
(42) Racine, S. C.; Davidson, E. R. *J. Phys. Chem.* **1993**, *97*, 6367.
(43) Frisch, M. J.; Trucks, G. W.; Schlegel, H. B.; Gill, P. M. W.; Johnson, B. G.; Robb, M. A.; Cheeseman, J. R.; Keith, T. A.; Petersson, G. A.; Montgomery, J. A.; Raghavachari, K.; Al-Laham, M. A.; Zakrzewski, V. G.; Ortiz, J. V.; Foresman, J. B.; Cioslowski, J.; Stefanov, B. B.; Nanayakkara, A.; Challacombe, M.; Peng, C. Y.; Ayala, P. Y.; Chen, W.; Wong, M. W.; Andres, J. L.; Replogle, E. S.; Gomperts, R.; Martin, R. L.; Fox, D. J.; Binkley, J. S.; Defrees, D. J.; Baker, J.; Stewart, J. P.; Head-Gordon, M.; Gonzalez, C.; Pople, J. A. *Gaussian 94*, rev. B.3; Gaussian, Inc.: Pittsburgh, PA, 1995.
(44) *MOLPRO* is a package of ab initio programs written by H.-J. Werner and P. J. Knowles with contribution from J. Almlof, R. D. Amos, M. J. O. Deegan, S. T. Elbert, C. Hampel, W. Meyer, K. Peterson, R. Pitzer, A. J. Stone, P. R. Taylor, and R. Lindh, 1996.
(45) Cybulski, S. M. *Trurl* 98 package; Oxford, OH, 1998.
(46) Sadlej, A. J. *Collect. Czech. Chem. Commun.* **1988**, *53*, 1995.
(47) Sadlej, A. J. *Theor. Chim. Acta* **1991**, *79*, 123.
(48) Vos, R. J.; van Lenthe, J. H.; van Duijneveldt, F. B. *J. Chem. Phys.* **1990**, *93*, 643.
(49) Vos, R. J.; Hendriks, R.; van Duijenveldt, F. B. *J. Comput. Chem.* **1990**, *11*, 1.
(50) van Duijenveldt-van de Rijdt, J. G. C. M.; van Duijenveldt, F. B. *J. Comput. Chem.* **1992**, *13*, 399.
(51) Tao, F.-M.; Pan, Y.-K. *J. Chem. Phys.* **1992**, *97*, 4989.
(52) *CRC Handbook of Chemistry and Physics*, 73rd ed.; Lide, D. R., Ed.; CRC Press: Boca Raton, FL, 1992.
(53) Packer, M. J.; Dalskov, E. K.; Sauer, S. P. A.; Oddershede, J. *Theor. Chim. Acta* **1994**, *89*, 323.
(54) Amos, R. D. *Chem. Phys. Lett.* **1982**, *87*, 23.
(55) Russell, A. J.; Spackman, M. A. *Mol. Phys.* **2000**, *98*, 633.
(56) Maroulis, G. *J. Chem. Phys.* **2000**, *113*, 1813.

(57) Wormer, P. E. S.; Hettema, H. *J. Chem. Phys.* **1992**, *97*, 5592.
(58) Clough, S. A.; Beers, Y.; Klein, G. P.; Rothman, L. S. *J. Chem. Phys.* **1973**, *59*, 2254.
(59) Flygare, W. H.; Benson, R. C. *Mol. Phys.* **1971**, *20*, 225.
(60) Maroulis, G. *J. Chem. Phys.* **1991**, *94*, 1182.
(61) Murphy, W. F. *J. Chem. Phys.* **1977**, *67*, 5877.
(62) Zeiss, G. D.; Meath, W. J. *Mol. Phys.* **1977**, *33*, 1155.
(63) Clark, W. W.; De Lucia, F. C. *J. Mol. Struct.* **1976**, *32*, 29.
(64) Wheatley, R. J. *Mol. Phys.* **1996**, *87*, 1083.
(65) Price, S. L.; Stone, A. J.; Alderton, M. *Mol. Phys.* **1984**, *52*, 987.
(66) Stone, A. J. *Mol. Phys.* **1978**, *36*, 241.
(67) Klopper, W.; van Duijenveldt-van de Rijdt, J. G. C. M.; van Duijenveldt, F. B. *Phys. Chem. Chem. Phys.* **2000**, *2*, 2227.
(68) Schütz, M.; Brdarski, S.; Widmark, P.-O.; Lindh, R.; Karlström, G. *J. Chem. Phys.* **1997**, *107*, 4597.